

See discussions, stats, and author profiles for this publication at: <https://www.researchgate.net/publication/336967380>

Water Retention, Air Exchange and Pore Structure Characteristics after Three Years of Rice Straw Biochar Application to an Acrisol

Article in *Soil Science Society of America Journal* · October 2019

DOI: 10.2136/sssaj2019.07.0230

CITATIONS

20

READS

373

7 authors, including:



Peter Bilson Obour
University of Ghana

52 PUBLICATIONS 1,040 CITATIONS

SEE PROFILE



E. Opong Danso
University of Ghana

30 PUBLICATIONS 199 CITATIONS

SEE PROFILE



Adam Yakubu
Iowa State University

11 PUBLICATIONS 82 CITATIONS

SEE PROFILE



Stephen Abenney-Mickson
Central University Accra Ghana

11 PUBLICATIONS 80 CITATIONS

SEE PROFILE

Water Retention, Air Exchange and Pore Structure Characteristics after Three Years of Rice Straw Biochar Application to an Acrisol

Peter Bilson Obour

Dep. of Agroecology, Faculty of Science and Technology
Aarhus Univ., PO Box 50
DK-8830 Tjele, Denmark

and

Dep. of Natural Resources and Environmental Sciences
Univ. of Illinois at Urbana-Champaign
1102 S. Goodwin Ave., MC-047
Urbana, IL 61801

Eric Opong Danso*

Adam Yakubu

Forest and Horticultural Crops Research Centre
School of Agriculture
Univ. of Ghana
PO Box LG 1195
Legon, Accra, Ghana

Stephen Abenney-Mickson

School of Engineering and Technology
Central Univ., PO Box, DS 2310
Dansoman, Accra, Ghana

Edward Benjamin Sabi

Dep. of Agricultural Engineering
School of Engineering Sciences
Univ. of Ghana, PO Box LG 77
Legon, Accra, Ghana

Yvonne Kugblenu Darrah

Soil and Irrigation Research Centre
School of Agriculture
Univ. of Ghana, PO Box LG 1195
Legon, Accra, Ghana

Emmanuel Arthur

Dep. of Agroecology, Faculty of Science and Technology
Aarhus Univ., PO Box 50
DK-8830 Tjele, Denmark

Biochar has been suggested as soil amendment for improving soil structure and associated functions for agricultural production. We investigated the impact of rice straw biochar application on soil water retention (SWR), air movement through soil, and soil pore characteristics of a tropical sandy clay loam field. A field experiment was conducted at the University of Ghana's Forest and Horticultural Crops Research Centre, Kade, Ghana, which comprised three treatments: soil without biochar (B0), and soil amended with 15 and 30 Mg ha⁻¹ of biochar (B15 and B30, respectively). Three years after biochar application, we sampled intact 100 cm³ soil cores and measured SWR, air permeability (k_a) and gas diffusivity (D_p/D_0), and quantified pore characteristics: tortuosity (τ), effective pore diameter (d_B) and the number of air-filled pores in a given soil cross-section (n_B) at selected matric potentials. At all matric potentials (–10 to –15000 hPa), B30 considerably reduced SWR compared to B0, whereas the B15 had similar SWR as B0. Biochar did not significantly affect the plant available water (PAW). The B30 significantly increased k_a at –30 hPa relative to B15. At a given air-filled porosity, the B30 tended to have larger D_p/D_0 values compared to B0. Despite these improvements in soil air transport, the effect of the biochar treatment was marginal on soil τ , d_B and n_B . We suggest that, probably higher biochar application rates and longer time are needed to significantly improve PAW and soil pore structure characteristics, which control air and gas transport through the soil.

Abbreviations: EC, electrical conductivity; FC, field capacity; PAW, plant available water; PO, pore organization; SOC, soil organic carbon; WP, wilting point.

Soil structure, which comprises the size and shape of soil pores is vital for maintaining agronomic productivity because it controls key soil functions, such as the storage and transport of water and nutrients as well as biota activity in soils. Soil pore spaces strongly determine the soil's capacity to exchange air between the soil matrix and the atmosphere. Information on soil pore structure characteristics can be derived from water retention characteristics and not least from the measurement of soil air and gas transport at each matric potential (Schjønning

Core Ideas

- Rice straw biochar was added to a sandy clay loam soil at 15 and 30 Mg ha⁻¹ (B15 and B30), respectively.
- B30 significantly reduced soil water content retained between –10 and –1000 hPa.
- Both B15 and B30 marginally increased plant available water content.
- Biochar tended to increase air permeability and pore size distributions at –50 to –300 hPa.
- Biochar did not significantly change the volume blocked air-filled pores.

Soil Sci. Soc. Am. J.
doi:10.2136/sssaj2019.07.0230
Received 29 July 2019.
Accepted 24 Sept. 2019.

*Corresponding author (eodanso@st.ug.edu.gh).

© 2019 The Author(s). Re-use requires permission from the publisher.

et al., 2002). The exchange of gas between soil and atmosphere occurs by convection and diffusion (Stepniewski, 2011). These two mechanisms can be, respectively, quantified by the air permeability (k_a) and relative gas diffusivity (D_p/D_0). Ball (1981) combined pore size distribution, k_a and D_p/D_0 to develop the tube model, which can be used to obtain quantitative information on three key pore characteristics: pore tortuosity (τ), effective pore diameter (d_B) and number of air-filled pores in a given soil cross-section (n_B). The d_B relates to gas transport characteristics and the τ parameter relates to pore continuity. Soil aeration is critical for plant growth and when soil air-filled porosity (ε_a), k_a and D_p/D_0 are below threshold levels, plant root growth and other biological activities are often negatively affected (Grable and Siemer, 1968). Ball et al. (1988) showed that quantitative information on 'blocked' pores, defined as air-filled pore space not taking part in the transport of air by convection or diffusion, together with the pore characteristics provide a useful indication of how different soil management practices impact on soil structural functions.

It is widely known that organic residues, applied directly or applied after charring into biochar, can positively affect soil pore structure and associated functions, which in turn improves soil quality for agricultural production. The practice of amending agricultural soils with biochar is gaining popularity due to its numerous benefits such as carbon sequestration, mitigation of greenhouse gas emissions and improvement in soil fertility for crop production (Dari et al., 2016; Nair et al., 2017; Sohi et al., 2010). Due to the lower particle density and highly porous structure of biochar compared to soils, its application alters not only soil chemical and biological properties, but also changes soil physical properties (Blanco-Canqui, 2017). Incorporation of biochar reduces soil bulk density and increases soil water retention capacity (e.g., Glab et al., 2016), although there are conflicting results from different studies (Atkinson, 2018; Glab et al., 2016; Omondi et al., 2016). For example, Fu et al. (2019) reported that, the application of biochar derived from corn straw and applied at a rate of 2.16% (w/w) to a loam soil increased plant available water (PAW). Similarly, Mollinedo et al. (2015) reported that a corn stover biochar applied at the rate of 4% (w/w) to a sandy loam soil significantly increased PAW relative to the control soil. On the contrary, Aller et al. (2017) found that the amendment of corn stover biochar at rate of 1% (w/w) decreased PAW in the sandy loam and clay loam soils, but found no change in the silt loam soil. The inconsistent results suggest the need for further research into biochar's effect on soil physical properties when introducing biochar as a soil conditioner for agricultural production.

Soil amendment with biochar also has the potential to modify soil structure and pore characteristics, which control air and gas transport through the soil as mentioned previously. However, research on biochar effects on air exchange in soils has also yielded variable results. For example, Sun et al. (2015) reported that the application of a wood-based biochar at a rate of 100 Mg ha⁻¹ to a sandy loam soil for 540 d increased the range of pore size distribution and τ of the soil pore network. More recently, Arthur and Ahmed (2017) found that the incorporation of rice straw biochar (3% w/w) into a sand-textured tropical soil significantly reduced k_a and D_p/D_0 after 450 d. Conversely, Amoakwah et al. (2017) did not find any significant difference between the biochar-amended and the control treatments for k_a and D_p/D_0 after 20 Mg ha⁻¹ of corn biochar was applied to a sandy loam soil for 180 d. There is a need for more research to adequately understand the mechanisms underlying biochar's impact on soil pore characteristics and functions.

The current study was therefore conducted to investigate the impact of rice straw biochar on the physical properties of a tropical sandy clay loam soil. The specific objectives were to examine how rice-straw biochar applied at different rates (i) impacts on soil water retention and air movement through the soil, and (ii) affects soil pore characteristics, such as pore organization and pore size distribution as well as τ , d_B and n_B . Findings of the study would contribute to the current literature on the importance of using rice straw biochar to improve soil physical properties for agricultural production, particularly soils in the humid tropics.

MATERIALS AND METHODS

Description of Study Area

The research was conducted at the University of Ghana's Forest and Horticultural Crops Research Centre, Kade (06°08'37" N, 00°54'10" W) located in the semi-deciduous agroecological zone of Ghana. The area has two rainfall seasons: a major rainy season between April and July, and minor rainy season between September and October, and a dry season from November to March. The area has an average annual rainfall and temperature of 1500 mm and 28°C, respectively. The texture of the soil is sandy clay loam and is classified as an Acrisol according to the WRB (2015) classification. Table 1 shows soil properties and water retention and aeration parameters measured prior to biochar application.

Experimental Set-up

Biochar Properties

The biochar was produced from rice straw feedstock that was pyrolyzed in a Lucia reactor at a temperature of 550°C for 48 h. The biochar produced was air-dried and subsequently passed through a 2-mm sieve prior to application. The physical

Table 1. Soil properties, water content held at field capacity (FC) and wilting point (WP), plant available water (PAW), air-filled porosity (ε_a), relative gas diffusivity (D_p/D_0) and air permeability (k_a) at -100 hPa measured before commencing the experiment.†

Clay	Silt	Sand	SOC	pH (H ₂ O)	EC	Water retention variable			ε_a	D_p/D_0 -100 hPa	k_a μm^2
						FC	WP	PAW			
%						$\mu\text{S cm}^{-1}$			$\text{m}^3 \text{m}^{-3}$		
21	11	68	1.33	5.54	36.0	0.26	0.15	0.11	0.14	0.009	7.20

† Clay: <0.002 mm, Silt: 0.002–0.02 mm, and Sand: 0.02–2 mm. SOC, soil organic carbon and EC, electrical conductivity.

and chemical properties of the biochar were: 92% dry matter, 25% total carbon, 1.0% total nitrogen, pH of 10.3, P, K, Ca, Mg, Fe and Na of 1420, 17700, 3020, 343, 2030, and 1250 mg kg⁻¹, respectively. The biochar had total poly-aromatic hydrocarbon content of 6 mg kg⁻¹.

Field Layout

The field experiment started in June 2015 and ended in May 2018. During the experimental period, we consecutively planted okra, maize, cowpea and maize in a randomized split plot design with four replicates. The main plots comprised three irrigation regimes of full, deficit and no irrigation with three biochar rates of 0, 15, and 30 Mg ha⁻¹ making up the sub-plots. Main plots had dimensions of 10.8 m by 5 m and subplots were 3.6 m by 5 m each. Sampling for the current study was performed only on the full irrigation treatments (i.e., 3 biochar levels × 4 replications = 12 plots in total). Application of biochar was split into three equal doses and applied in June 2015, June 2016 and June 2017. For each round of split application, biochar at rates of 0, 5, and 10 Mg ha⁻¹ was surface-applied and incorporated into the soil at a depth of about 15 cm using a hoe and a rake. Thus, the total applied biochar prior to sampling for the present study added up to 0 Mg ha⁻¹, 15 Mg ha⁻¹, and 30 Mg ha⁻¹, corresponding to 0, 0.66 and 1.32% by weight. The treatments 0, 15, and 30 Mg ha⁻¹ hereafter, are designated B0, B15 and B30, respectively.

Sampling

Soil sampling was done in May 2018 after the harvest of the last crop (maize). To avoid soil disturbance and the root mat in the uppermost layer, intact soil cores were sampled from all the 12 experimental plots at a depth of 10 to 15 cm using metal core samplers (6.1 cm diameter, 3.4 cm high, 100 cm³). Sampling was done in the center of the plots and avoided visibly compacted areas. Four replicate samples were taken from each plot, except in one of the control plots where only three replicate samples were taken due to technical difficulties. In total, 47 intact soil cores were sampled and used for water retention, k_a and gas diffusion measurements. In addition, 12 bulk samples (1 sample × 4 replication × 3 treatments) were sampled from the same depth as the soil cores. The bulk samples were pooled together for each treatment. The bulk samples were then air-dried at 25°C and sieved to <2 mm prior to determination of soil texture, organic matter, pH, water content at wilting point and electrical conductivity.

Measurements

Soil Chemical Properties

The particle size distribution of the samples were measured by wet sieving and hydrometer method (Gee and Or, 2002). Total carbon was determined through oxidation of carbon to CO₂ at 950°C with a FLASH 2000 organic elemental analyzer coupled to a thermal conductivity detector (Thermo Fisher Scientific, MA, USA). The samples were devoid of calcium carbonates, hence the total carbon equaled the soil organic carbon (SOC). To determine soil pH, 10 g of air-dried soil sample was

mixed with 25 mL of deionized water (1:2.5). The mixture was shaken for 10 min, and allowed to settle for 10 min. The pH was measured with a pH meter (PHM220, Radiometer Analytical SAS, Lyon). Soil EC was determined by adding 4 g of air-dried soil sample to 36 mL of deionized water, shaken for 1 h and settled for 1 h before the EC was determined with an EC meter (CDM210, Radiometer Analytical SAS, Lyon).

Soil Water Retention

The soil water retention curve from -10 to -1000 hPa matric potential was determined using sandboxes, vacuum pots and pressure plates. Briefly, the soil cores were placed in a sandbox and slowly saturated by capillary action with water from below to remove any entrapped air. Thereafter, the samples were drained stepwise to matric potentials of -10, -30, -50 and -100 hPa. For the matric potentials of -300, -500 and -1000 hPa, vacuum pots and pressure plates were used following the procedure described by Dane and Hopmans (2002). The water content at -15000 hPa matric potential was measured on the air-dried <2 mm samples using a WP4-T dewpoint potentiometer following the method by Scanlon et al. (2002). Plant available water (PAW) was calculated as the difference between water content retained at -300 hPa (field capacity, FC) and water content retained at -15000 hPa (wilting point, WP).

Air Permeability and Gas Diffusion

Air permeability (k_a) and the soil gas diffusion coefficient (D_p) were measured on the soil cores at -30, -50, -100 and -300 hPa. The k_a was measured following the Forchheimer approach described in Schjønning and Koppelgaard (2017). The D_p was measured according to Taylor (1949) using an apparatus developed by Schjønning (1985). Relative gas diffusivity (D_p/D_0) was quantified as the ratio of D_p to the gas diffusion in free air (D_0).

Bulk Density and Air-Filled Porosity

After draining the soil cores at -1000 hPa matric potential, they were oven dried at 105°C for 24 h. Soil bulk density was estimated as the ratio of the oven-dried mass to the total volume of each soil core. The total porosity was calculated from bulk density and an assumed particle density of 2.65 Mg m⁻³. The volumetric water content at each matric potential was estimated by multiplying the gravimetric water content by bulk density. The air-filled porosity (ϵ_a) was estimated as the difference between total porosity and volumetric water content at a given matric potential.

Modeling of Soil Pore Size Distribution and Architecture

The pore size distributions of the soil were calculated from the water retention measurements as:

$$d = -3000 / \psi \quad [1]$$

where d is equivalent cylindrical pore diameter (μm) and ψ is the soil matric potential (hPa).

Table 2. Chemical and physical properties for B0 (0 Mg ha⁻¹), and soil amended with biochar: B15 (15 Mg ha⁻¹) and B30 (30 Mg ha⁻¹).

Property	B0	B15	B30
Clay, <0.002 mm (%)	23 (0.45)†	22 (0.52)	19 (1.02)
Silt, 0.002–0.02 mm (%)	10 (0.29)	10 (0.39)	10 (0.35)
Sand, 0.02–2 mm (%)	66 (0.18)	68 (0.63)	70 (1.10)
Soil organic carbon (%)	1.04 (0.05) b‡	1.12 (0.08) ab	1.48 (0.10) a
pH, H ₂ O	4.66 (0.08) b	5.14 (0.20) ab	5.55 (0.05) a
EC (μS cm ⁻¹)	17.0 (0.52) b	21.6 (3.67) ab	37.0 (6.10) a
Bulk density (g cm ⁻³)	1.51 (0.03)	1.54 (0.03)	1.49 (0.02)

† Numbers in parentheses are standard errors of the mean ($n = 4$).

‡ Treatments without a common letter in a given row for each soil attribute are significantly different at $p < 0.05$.

The relationship between k_a and ε_a was used to estimate two indices of pore continuity: $PO_1 = k_a / \varepsilon_a$ and $PO_2 = k_a / \varepsilon_a^2$ (Groenevelt et al., 1984). The two parameters PO_1 and PO_2 describe the soil pore organization according to Blackwell et al. (1990). The k_a was related to ε_a by a logarithmic form of the exponential model proposed by Millington and Quirk (1961):

$$\log(k_a) = \log(M) + N \log(\varepsilon_a) \quad [2]$$

where M and N are constants reflecting soil pore characteristics. N is a pore continuity index indicating the rate of opening of continuous pore air paths with decreasing matric potential (Ball et al., 1988). An estimate of blocked air-filled pore space (ε_b) was computed from the model as $10^{-\log(M)/N}$ (Ball et al., 1988). Similarly, D_p/D_0 was related to ε_a by a logarithmic form of the exponential model proposed by Marshall (1959):

$$\log(D_p/D_0) = \log(m) + n \log(\varepsilon_a) \quad [3]$$

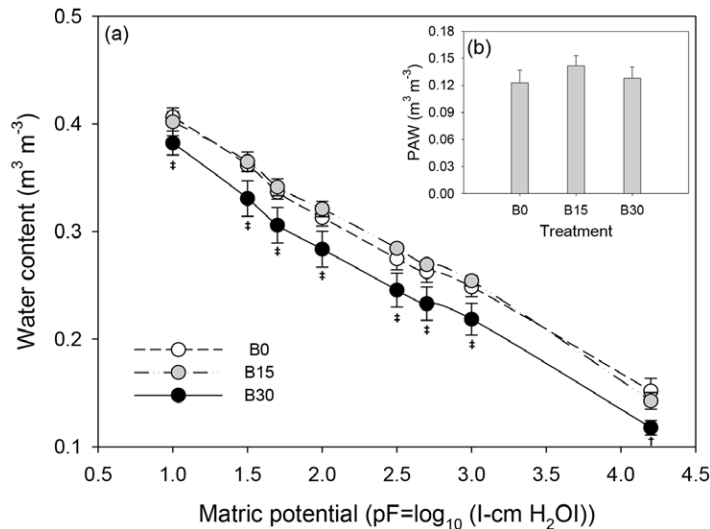


Fig. 1. (a) Water content at given matric potential (pF 1.0–4.2) for B0, control (0 Mg ha⁻¹), and soil amended with biochar: B15 (15 Mg ha⁻¹) and B30 (30 Mg ha⁻¹). (b) Plant available water (PAW) for the B0, B15 and B30 treatments. ‡ indicates B30 is significantly lower ($p < 0.05$) than both B0 and B15, † indicates B30 is significantly lower than only B0. Error bars indicate standard errors of the mean ($n = 4$).

where m and n are constants. As for k_a , an estimate of ε_b was computed from the model as $10^{-(\log(m)+4)/n}$.

The tube model of Ball (1981) was used to quantify soil pore tortuosity (τ), effective pore diameter (d_B), and the number of air-filled pores in a soil cross-section (n_B):

$$\tau = \left\{ \frac{\varepsilon_a}{D_p/D_0} \right\}^{1/2} \quad [4]$$

$$d_B = 2 \left\{ \frac{8k_a}{D_p/D_0} \right\}^{1/2} \quad [5]$$

$$n_B = \frac{\varepsilon_a^{1/2} (D_p/D_0)^{3/2}}{8\pi k_a} \quad [6]$$

Statistical Analyses

Prior to all statistical analyses, the non-normally distributed variables, k_a , PO_1 and PO_2 data were logarithmically (ln) transformed to ensure normality. Statistical analyses were performed on the data using the R software package version 3.4.1 (R Core Team, 2017). To analyze the effect of treatment, data were fitted by a linear mixed effects model including treatment as fixed and block as random factors. The criterion used for statistical significance of treatment effect was $p < 0.05$. An ANOVA test was performed to ascertain the significance of treatment. When the treatment effect was significant, further analyses were performed to identify which treatments means were different by performing a pairwise comparison using the general linear hypotheses (*glht*) function from the R *multcomp* package and Tukey's Honest Significant Difference (Tukey's HSD) test.

RESULTS

Soil Chemical and Physical Properties after Biochar Amendment

The soil texture, soil organic carbon (SOC), pH, electrical conductivity (EC) and bulk density of the treatment plots are presented in Table 2. Clay content for the B0 and B15 treatments was slightly higher compared to the B30 treated soil. The sand content showed the opposite trend. Silt content was identical for all the treatments. The SOC, pH and EC were significantly higher for the B30 compared to the B0 and B15. The B15 treatment did not statistically differ from B0 for any of the soil chemical properties. Further, bulk density for B15 and B30 was statistically similar to B0.

Soil Water Retention Characteristics

The B30 treatment had lower water content at all the matric potentials compared to B0 and B15, except at -15000 hPa, where it was significantly lower than B0 (Fig. 1a). Conversely, the water content for the B15 did not statistically differ from the B0 at any of the matric potentials. Biochar application of 15 and 30 Mg ha⁻¹ did not significantly increase the plant available water (PAW) relative to B0 (Fig. 1b).

Table 3. Air permeability (k_a) and pore organization indices ($PO_1 = k_a/\varepsilon_a$ and $PO_2 = k_a/\varepsilon_a^2$) at four matric potentials for the B0, control (0 Mg ha⁻¹), and soil amended with biochar: B15 (15 Mg ha⁻¹) and B30 (30 Mg ha⁻¹).

Matric potential	k_a			PO_1			PO_2		
	B0	B15	B30	B0	B15	B30	B0	B15	B30
hPa	mm ²								
-30	5.6 [0.51] ab†‡	5.0 [0.30] b	16.2 [0.49] a	88 [0.34]	114 [0.54]	179 [0.32]	1848 [0.34]	3273 [0.28]	1814 [0.16]
-50	7.5 [0.47]	7.8 [0.44]	22.0 [0.47]	102 [0.32]	134 [0.47]	171 [0.30]	1040 [0.30]	4453 [0.69]	1463 [0.19]
-100	8.8 [0.47]	11.1 [0.49]	27.8 [0.47]	80 [0.34]	122 [0.54]	190 [0.34]	734 [0.27]	1344 [0.61]	1291 [0.22]
-300	14.0 [0.39]	18.5 [0.56]	35.1 [0.43]	94 [0.30]	142 [0.57]	188 [0.34]	628 [0.27]	1086 [0.57]	1003 [0.25]

† Numbers in square brackets indicate standard errors of the mean ($n = 4$) for the log-transformed (\ln) data.

‡ Treatments labeled with different letters in a given row for k_a , PO_1 and PO_2 are significantly different at $p < 0.05$.

Air Permeability and Soil Pore Size Distributions

The addition of biochar led to increased k_a at -30 , -50 , -100 and -300 hPa matric potentials (150 to 215% increases for the B30 treatment), although the increases were not significant except at -30 hPa, where the B30 was significantly higher than B15 (Table 3). In addition, B15 and B30 insignificantly increased pore organization indices (PO_1 and PO_2) compared to the no biochar-amended soil (Table 3). At -100 hPa, B15 increased PO_1 and PO_2 by 52 and 83%, respectively, whereas the B30 increased by 136 and 76%.

Gas Diffusivity

Relative gas diffusivity (D_p/D_0) as a function of air-filled porosity (ε_a) at -30 , -50 , -100 and -300 hPa is illustrated in Fig. 2. For all the treatments, D_p/D_0 increased with increasing ε_a . Biochar application did not significantly affect ε_a and D_p/D_0 for the range of matric potentials considered (-30 to -300 hPa). However, there was a trend showing that at any given matric potential, the B30 treatment increased both ε_a and D_p/D_0 compared to B15. In fact, the B15 consistently had low ε_a at -30 , -50 , -100 , and -300 hPa (Fig. 2).

Model-Derived Pore Characteristics

Morphological Characteristics across Matric Potentials

Biochar application did not significantly affect tortuosity of pores (τ) and effective pore diameter (d_B) at any of the matric potentials considered (Fig. 3a and b). However, B30 consistently decreased τ compared to B0. Conversely, the B15 treatment consistently, but marginally increased τ compared to B0. The B15 and B30 treatments increased d_B compared to the B0 treatment, but the difference was not significant at any of the matric potentials considered. The B30 significantly increased the number of air-filled pores in a given soil cross-section (n_B) at -30 and -50 hPa compared to the B15 (Fig. 3c).

Blocked Soil Air-Filled Pore Space across Matric Potentials

The regression parameters obtained from k_a vs. ε_a and D_p/D_0 vs. ε_a at four matric potentials corresponding to the logarithmic form of the exponential model in Eq.

[2] and [3] are shown in Table 4. For all the treatments, there was a strong linear and positive relationship between D_p/D_0 vs. ε_a , and k_a vs. ε_a , shown by the large coefficient of determination (R^2). The n parameter was slightly higher for B30 compared to the B0 soil. The highest biochar rate of 30 Mg ha⁻¹ only marginally increased blocked air-filled pore space (ε_b), whereas the B15 decreased ε_b compared to B0 and B30 albeit insignificant. Unlike D_p/D_0 vs. ε_a , the regression parameters from the exponential model derived from k_a vs. ε_a showed that the N parameter marginally increased for the biochar amended soils compared to the control. The B15 treatment slightly increased ε_b , with B0 and B15 having identical ε_b (Table 4).

DISCUSSION

Biochar and Soil Water Retention Variables

Soil water retention is a key soil hydraulic property governing soil functions and strongly influences soil productivity. Application of biochar can modify soil water retention characteristics (Laird et al., 2010; Wang et al., 2019). Due to its higher porosity and high absorptive capacity for water, biochar amendment can increase soil water retention resulting in increased plant

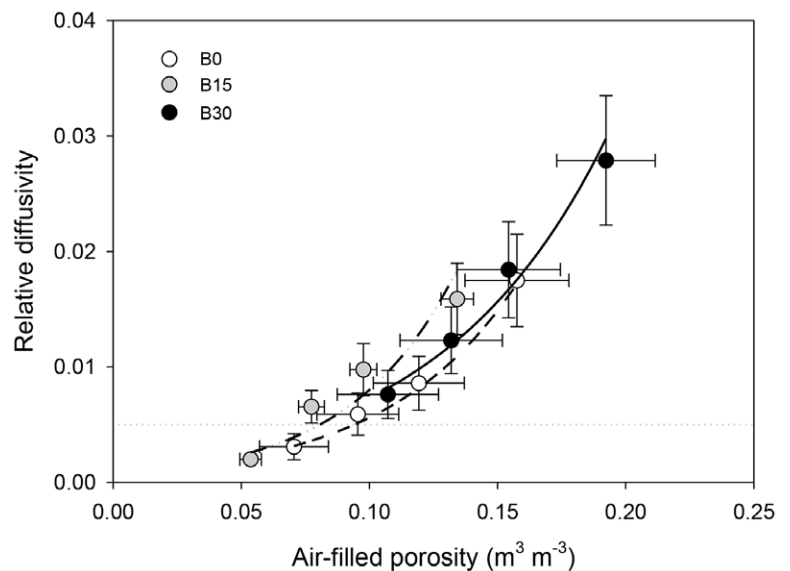


Fig. 2. Relative gas diffusivity as a function of air-filled porosity, calculated from total porosity and water retained at -30 , -50 , -100 and -300 hPa for the B0, control (0 Mg ha⁻¹), and soil amended with biochar: B15 (15 Mg ha⁻¹) and B30 (30 Mg ha⁻¹). Dotted horizontal line indicates lower threshold value for relative gas diffusivity. Error bars indicate standard errors of the mean ($n = 4$).

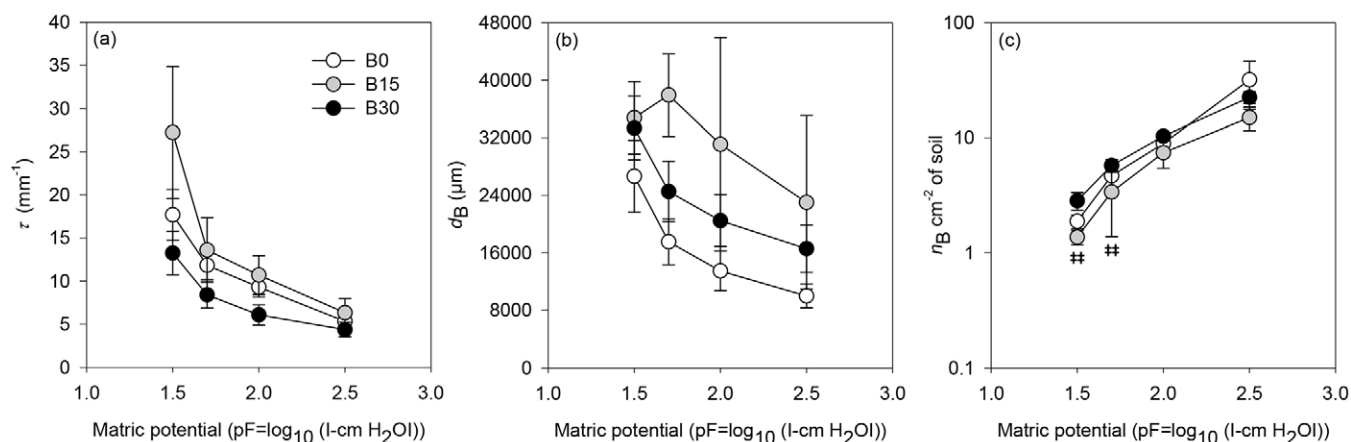


Fig. 3. (a) Estimate of pore tortuosity (τ), (b) effective pore diameter (d_B) and (c) number of soil pores in a given soil cross-section (n_B) derived using the tube model of Ball (1981) at -30 , -50 , -100 and -300 hPa for the B0, control (0 Mg ha^{-1}), and soil amended with biochar: B15 (15 Mg ha^{-1}) and B30 (30 Mg ha^{-1}). ## indicates B30 is significantly different ($p < 0.05$) only from B15. Error bars indicate standard errors of the mean ($n = 4$).

available water (PAW) (Blanco-Canqui, 2017). However, the magnitude of increase depends on biochar attributes, experimental conditions and soil properties (Blanco-Canqui, 2017; Omondi et al., 2016). Results showed that biochar application of 30 Mg ha^{-1} significantly reduced the water content held at field capacity (FC) (Fig. 1a). We postulate that high FC for the B15 is possibly because the lower biochar application might have caused the biochar particles to occupy the soil pores, which in turn reduced the soil pore size. The presence of large proportion of smaller pores in the B15 might have enhanced water storage compared to the B30. Biochar decreased soil water content held at wilting point (WP) compared to the control soil, although significant only for B30 (Fig. 1a). However, neither the B15 nor B30 treatments significantly increased PAW relative to the control (Fig. 1b).

Impact of Biochar on Soil Functions and Soil Structural Complexity

Air and Gas Transportation

Soil aeration is a critical element for crop development, and the ability of a soil to conduct air is a crucial requirement for crop productivity. Movement of air through soil is governed by soil physical properties such as the fraction of water and air-filled pore space, and pore characteristics, e.g., pore size and continuity. A soil with k_a as low as $1 \mu\text{m}^2$ may be regarded effectively impermeable (Ball et al., 1988). Unlike k_a , the critical and limiting value of D_p/D_0 for plant growth is variable. Since the diffusion rate in air is $\sim 10^4$ times that in water, the D_p/D_0 threshold for plant growth has been estimated to range from 0.005 to 0.02 (Stepniewski,

1981). Results showed that, although not significant, the B30 treatment increased ϵ_a , D_p/D_0 and k_a (Fig. 2; Table 3) by 29, 114, and 215% relative to B0 at -100 hPa. At -30 hPa, the B15 and B0 had D_p/D_0 values as low as 0.003 and 0.002, respectively, which are below the critical limit for plant growth. Deficient aeration conditions in soil could restrict processes such as root and microorganism respiration, and water and nutrient absorption (Neira et al., 2015). It can also create anaerobic microsites, which contribute to the emission of greenhouse gases such as N_2O and CH_4 (Munoz et al., 2010). Due to its porous nature, biochar increases the fraction of pore space in soil. Sun et al. (2013) reported that the application of 20 Mg ha^{-1} birch wood biochar increased ϵ_a by 28 to 34%, 53 to 161% for D_p/D_0 and 69 to 223% for k_a . The increased soil aeration following biochar application in the B30 treatment is consistent with the literature. Conversely, at all the matric potentials considered, the B15 treatment had similar ϵ_a , D_p/D_0 and k_a as the B0; this implies that the application of rice straw biochar at a relatively low rate ($\leq 15 \text{ Mg ha}^{-1}$) may be inadequate to positively impact the aeration of sandy clay loams.

Pore Characteristics

The pore organization indices ($PO_1 = k_a/\epsilon_a$ and $PO_2 = k_a/\epsilon_a^2$) are useful for evaluating soil structural differences. Soils with similar PO_1 have similar pore size distributions and pore continuities, whereas soils that have similar PO_2 values have similar pore size distributions but not necessarily similar pore continuities. Thus, the difference between PO_1 and PO_2 relates to differences in pore continuity (Groenevelt et al., 1984). No significant dif-

Table 4. Results from the model expressed by relating relative gas diffusivity (D_p/D_0) or air permeability (k_a) to air-filled pore volume at a range of matric potentials (-30 to -300 hPa) for B0, control (0 Mg ha^{-1}), and soil amended with biochar: B15 (15 Mg ha^{-1}) and B30 (30 Mg ha^{-1}). The values $10^{-(\log(m)+4)/n}$ and $10^{-\log(M)/N}$ are model predictions of blocked air-filled pore space ($\text{m}^3 \text{ m}^{-3}$) at $D_p/D_0 = 10^{-4}$ and $k_a = 1 \mu\text{m}^2$ (Ball et al., 1988).

Treatment	Model predictions: $\log(D_p/D_0) = \log(m) + n \log(\epsilon_a)$				Model predictions: $\log(k_a) = \log(M) + N \log(\epsilon_a)$			
	$\log(m)$	n	R^2	$10^{-(\log(m)+4)/n}$	$\log(M)$	N	R^2	$10^{-\log(M)/N}$
B0	-0.05 (0.19)†	2.19 (0.21)	0.98	0.016 (0.004)	2.09 (0.28)	0.97 (0.26)	0.92	0.012 (0.004)
B15	0.08 (0.23)	2.13 (0.12)	0.95	0.012 (0.001)	3.41 (0.91)	1.91 (0.60)	0.83	0.015 (0.004)
B30	0.12 (0.20)	2.37 (0.29)	1.00	0.019 (0.005)	2.78 (0.28)	1.40 (0.28)	0.99	0.012 (0.004)

† Numbers in parenthesis are standard errors of the mean.

ference was found for PO_1 and PO_2 between the biochar treated soils and the control. Both PO_1 and PO_2 tended to increase with biochar for the matric potentials range from -30 to -300 hPa (Table 3). Similarly, for a sandy loam, application of 20 Mg ha^{-1} corn cob biochar to a sandy loam soil did not induce any measurable changes in PO_1 after 6 mo (Amoakwah et al., 2017)

The pore characteristics computed from the tube model of Ball (1981) may be interpreted as indices of the soil pore system. Neither biochar application amount of 15 nor 30 Mg ha^{-1} significantly changed τ and d_B of the soil (Fig. 3a and b). However, the B30 significantly increased n_B at -30 and -50 compared to the B15, which could be attributed to a reduction in soil pore size for the latter treatment as mentioned previously.

The relationship between k_a and ϵ_a can be used to identify changes in soil structure induced by management practices (Blackwell et al., 1990). The structural changes with respect to pore organization (PO_1 and PO_2) have been discussed above. As for k_a/ϵ_a , the relationship between D_p/D_0 and ϵ_a can be used to describe pore continuity and tortuosity (Ball, 1981). The regression parameters n and N parameters (Table 4) obtained from D_p/D_0 and k_a as a function of ϵ_a showed the rate of opening of pathways for air transport with increasing air-filled pore space (Dörner et al., 2012; Schjønning et al., 2002). Results here showed that after 3 yr of biochar amendment, the rice straw biochar used in our study did not significantly affect the n and N parameters as well as the blocked air-filled porosity. However, both the B15 and B30 increased the N parameter at -30 to -300 hPa relative to the B0 treatment (Table 4). From a practical point of view, these findings indicate that high biochar application rates and probably even longer time may be required for the rice straw biochar to considerably change the structure and pore characteristics of the sandy clay loam soil.

CONCLUSIONS

Soil water retention, aeration parameters and pore structure characteristics of a tropical sandy clay loam soil amended with a rice straw biochar at rates of 0, 15, and 30 Mg ha^{-1} (B0, B15 and B30, respectively) were compared. We showed that after 3 yr of biochar incorporation, the B30 treatment consistently and significantly reduced water retention capacity at -10 to -1000 hPa compared to the B0 and B15 treatments. Biochar application also slightly increased air permeability and pore size distributions and/or continuity at -50 to -300 hPa. The impact of biochar on pore morphological characteristics such as pore tortuosity, effective pore diameter and the number of air-filled pores in a soil cross-section did not show any clear trends. For practical significance, findings suggest that high biochar application rates or even longer time or both may be required before the rice straw biochar induces any measurable changes in physical properties of the investigated soil.

ACKNOWLEDGMENTS

The study was funded by Danida (Ministry of Foreign Affairs of Denmark) through "Green Cohesive Agricultural Resource Management, WEBSOC", DFC project no. 13-01AU and by VILLUM FONDEN research grant no. 13162. The assistance of Bodil B. Christensen with the soil water retention and air permeability measurements is also duly acknowledged.

REFERENCES

- Aller, D., S. Rathke, D. Laird, R. Cruse, and J. Hatfield. 2017. Impacts of fresh and aged biochars on plant available water and water use efficiency. *Geoderma* 307:114–121. doi:10.1016/j.geoderma.2017.08.007
- Amoakwah, E., K.A. Frimpong, D. Okae-Anti, and E. Arthur. 2017. Soil water retention, air flow and pore structure characteristics after corn cob biochar application to a tropical sandy loam. *Geoderma* 307:189–197. doi:10.1016/j.geoderma.2017.08.025
- Arthur, E., and F. Ahmed. 2017. Rice straw biochar affects water retention and air movement in a sand-textured tropical soil. *Arch. Agron. Soil Sci.* 63:2035–2047. doi:10.1080/03650340.2017.1322196
- Atkinson, C.J. 2018. How good is the evidence that soil-applied biochar improves water-holding capacity? *Soil Use Manage.* 34:177–186. doi:10.1111/sum.12413
- Ball, B.C. 1981. Modelling of soil pores as tubes using gas permeabilities, gas diffusivities and water release. *Eur. J. Soil Sci.* 32:465–481. doi:10.1111/j.1365-2389.1981.tb01723.x
- Ball, B.C., M.F. O'Sullivan, and R. Hunter. 1988. Gas-diffusion, fluid-flow and derived pore continuity indexes in relation to vehicle traffic and tillage. *J. Soil Sci.* 39:327–339. doi:10.1111/j.1365-2389.1988.tb01219.x
- Blackwell, P.S., A.J. Ringrose-Voase, N.S. Jayawardane, K.A. Olsson, D.C. McKenzie, and W.K. Mason. 1990. The use of air-filled porosity and intrinsic permeability to air to characterize structure of macropore space and saturated hydraulic conductivity of clay soils. *Soil Sci.* 41:215–228. doi:10.1111/j.1365-2389.1990.tb00058.x
- Blanco-Canqui, H. 2017. Biochar and Soil Physical Properties. *Soil Sci. Soc. Am. J.* 81:687–711. doi:10.2136/sssaj2017.01.0017
- Dane, J.H., and J.W. Hopmans. 2002. Water retention and storage. In: J.H. Dane and G.C. Topp, editors, *Methods of soil analysis. Part 4. Physical methods.* SSSA, Madison, WI. p. 671–796.
- Dari, B., V.D. Nair, W.G. Harris, P.K.R. Nair, L. Sollenberger, and R. Mylavarapu. 2016. Relative influence of soil- vs. biochar properties on soil phosphorus retention. *Geoderma* 280:82–87. doi:10.1016/j.geoderma.2016.06.018
- Dörner, J., D. Dec, E. Feest, N. Vasquez, and M. Diaz. 2012. Dynamics of soil structure and pore functions of a volcanic ash soil under tillage. *Soil Tillage Res.* 125:52–60. doi:10.1016/j.still.2012.05.019
- Fu, Q., H. Zhao, T. Li, R. Hou, D. Liu, Y. Ji, Z. Zhou, and L. Yang. 2019. Effects of biochar addition on soil hydraulic properties before and after freezing-thawing. *Catena* 176:112–124. doi:10.1016/j.catena.2019.01.008
- Gee, G.W., and D. Or. 2002. Particle-size analysis. In: J.H. Dane and C.G. Topp, editors, *Methods of soil analysis: Part 4. Physical methods.* SSSA, Madison, WI. p. 255–293.
- Glab, T., J. Palmowska, T. Zaleski, and K. Gondek. 2016. Effect of biochar application on soil hydrological properties and physical quality of sandy soil. *Geoderma* 281:11–20. doi:10.1016/j.geoderma.2016.06.028
- Grable, A.R., and E.G. Siemer. 1968. Effects of bulk density aggregate size and soil water suction on oxygen diffusion redox potentials and elongation of corn roots. *Soil Sci. Soc. Am. Proc.* 32:180–186. doi:10.2136/sssaj1968.03615995003200020011x
- Groenevelt, P.H., B.D. Kay, and C.D. Grant. 1984. Physical assessment of a soil with respect to rooting potential. *Geoderma* 34:101–114. doi:10.1016/0016-7061(84)90016-8
- Laird, D.A., P. Fleming, D.D. Davis, R. Horton, B.Q. Wang, and D.L. Karlen. 2010. Impact of biochar amendments on the quality of a typical Midwestern agricultural soil. *Geoderma* 158:443–449. doi:10.1016/j.geoderma.2010.05.013
- Marshall, T.J. 1959. The diffusion of gases through porous media. *J. Soil Sci.* 10:79–82. doi:10.1111/j.1365-2389.1959.tb00667.x
- Millington, R.J., and J.M. Quirk. 1961. Permeability of porous solids. *Trans. Faraday Soc.* 57:1200–1207. doi:10.1039/tf9615701200
- Mollinedo, J., T.E. Schumacher, and R. Chintala. 2015. Influence of feedstocks and pyrolysis on biochar's capacity to modify soil water retention characteristics. *J. Anal. Appl. Pyrolysis* 114:100–108. doi:10.1016/j.jaap.2015.05.006
- Munoz, C., L. Paulino, C. Monreal, and E. Zagal. 2010. Greenhouse gas (CO_2 and N_2O) emissions from soils: A review. *Chil. J. Agric. Res.* 70:485–497. doi:10.4067/S0718-58392010000300016
- Nair, V.D., P.K.R. Nair, B. Dari, A.M. Freitas, N. Chatterjee, and F.M. Pinheiro. 2017. Biochar in the agroecosystem–climate-change–sustainability nexus. *Front. Plant Sci.* 8:1–9.

- Neira, J., M. Ortiz, L. Morales, and E. Acevedo. 2015. Oxygen diffusion in soils: Understanding the factors and processes needed for modeling. *Chil. J. Agric. Res.* 75:35–44. doi:10.4067/S0718-58392015000300005
- Omondi, M.O., X. Xia, A. Nahayo, X.Y. Liu, P.K. Korai, and G.X. Pan. 2016. Quantification of biochar effects on soil hydrological properties using meta-analysis of literature data. *Geoderma* 274:28–34. doi:10.1016/j.geoderma.2016.03.029
- R Core Team. 2017. R: A language and environment for statistical computing, R Foundation for Statistical Computing, Vienna, Austria. <https://www.R-project.org/>.
- Scanlon, B.R., B.J. Andraski, and J. Bilskie. 2002. Miscellaneous methods for measuring matric or water potential. In: J.H. Dane and G.C. Topp, editors, *Methods of soil analysis: Part 4. Physical methods*. SSSA, Madison, WI. p. 643–670.
- Schjønning, P. 1985. A laboratory method for determination of gas diffusion in soil. Danish Institute of Plant and Soil Science, Tjele, Denmark.
- Schjønning, P., and M. Koppelgaard. 2017. The Forchheimer approach for soil air permeability measurement. *Soil Sci. Soc. Am. J.* 81:1045–1053. doi:10.2136/sssaj2017.02.0056
- Schjønning, P., L.J. Munkholm, P. Moldrup, and O.H. Jacobsen. 2002. Modeling soil pore characteristics from measurements of air exchange: The long-term effects of fertilization and crop rotation. *Eur. J. Soil Sci.* 53:331–339. doi:10.1046/j.1365-2389.2002.00438.x
- Sohi, S.P., E. Krull, E. Lopez-Capel, and R. Bol. 2010. A review of biochar and its use and function in soil. *Adv. Agron.* 105:47–82. doi:10.1016/S0065-2113(10)05002-9
- Stepniewski, W. 1981. Oxygen diffusion and strength as related to soil compaction: II. Oxygen diffusion coefficient. *Pol. J. Soil Sci.* 14:3–13.
- Stepniewski, W. 2011. Aeration of soils and plants. In: J. Gliński, J. Horabik, and J. Lipiec, editors, *Encyclopedia of agrophysics*. Springer, Dordrecht, Netherlands. p. 8–14. doi:10.1007/978-90-481-3585-1_6
- Sun, Z., E. Arthur, L.W. de Jonge, L. Elsgaard, and P. Moldrup. 2015. Pore structure characteristics after 2 years of biochar application to a sandy loam field. *Soil Sci.* 180:41–46. doi:10.1097/SS.0000000000000111
- Sun, Z., P. Moldrup, L. Elsgaard, E. Arthur, and E.W. Bruun. 2013. Direct and indirect short-term effects of biochar on physical characteristics of an arable sandy loam. *Soil Sci.* 178:465–473. doi:10.1097/SS.0000000000000010
- Taylor, S.A. 1949. Oxygen diffusion in porous media as a measure of soil aeration. *Soil Sci. Soc. Am. Proc.* 14:55–60. doi:10.2136/sssaj1950.036159950014000C0013x
- Wang, D., C. Li, S.J. Parikh, and K.M. Scow. 2019. Impact of biochar on water retention of two agricultural soils— A multi-scale analysis. *Geoderma* 340:185–191. doi:10.1016/j.geoderma.2019.01.012
- WRB. I.W.G., 2015. World Reference Base for soil resources 2014, update 2015. International soil classification system for naming soils and creating legends for soil maps, World Soil Resources Reports No. 106. FAO, Rome.